

STUDIES ON THE EXERGY LOSS STRUCTURE OF SOME FUNDAMENTAL TURBULENT FLOWS

Dorin STANCIU¹, Alexandru DOBROVICESCU²,
Camelia PETRE³, Horatiu POP⁴

Creșterea eficienței exergetice a proceselor termice este întotdeauna strâns legată de reducerea ireversibilităților. Adeseori procesele termodinamice sunt realizate de curgeri turbulente complexe, a căror configurație este formată din unul sau mai multe straturi limită, jeturi libere sau însoțite, dârere, zone de recirculare, etc. Obiectivul acestei lucrări este acela de a evidenția structura pierderilor exergetice pentru astfel de curgeri elementare. Utilizând abordarea intrinsecă a metodei exergetice, a rezultat că disipațiile turbulente au un rol esențial în structura pierderilor de exergie în statul limită turbulent și sunt aproape în totalitate responsabile pentru distrugerea exergiei în jeturi și dârările turbulente. Aceste rezultate pot fi utile în efortul de îmbunătățire a eficienței exergetice a proceselor termodinamice.

The improvement in exergy efficiency of thermal processes is always linked with the irreversibility reduction. Very often, the thermal processes are performed by complex turbulent flows, whose configuration contains boundary and mixing layers, wakes, recirculation zones, etc. The goal of this paper is to investigate the structure of exergy destruction for these types of fundamental turbulent flows. Using the intrinsic approach of exergy analysis we found that the turbulent dissipations play an essential role in the exergy lost structure of wall attached layers and they are almost totally responsible for the exergy destruction in the free shear flows. These results could help in the future for improving the exergy efficiency of thermal processes by operating regimes and geometrical shape modifications.

Keywords: entropy generation, exergy destruction, intrinsic level of analysis.

1. Introduction

The second law and the exergy analysis become the most currently used methods to evaluate thermal processes efficiency. Often, they are combined with the thermo-economic analysis that balance the investment needed to achieve thermodynamic efficiency increase and its effects on the economic revenue.

¹ Reader, Dept. of Engineering Thermodynamics, University POLITEHNICA Bucharest, Romania, e-mail: sdorin_ro@yahoo.com

² Prof., Dept. of Engineering Thermodynamics, University POLITEHNICA Bucharest, Romania

³ Lecturer., Dept. of Engineering Thermodynamics, University POLITEHNICA Bucharest, Romania

⁴ Assist., Dept. of Engineering Thermodynamics, University POLITEHNICA Bucharest, Romania

Basically, these methods cannot be separated because all of them involve in an explicit or implicit manner the Gouy- Stodola theorem.

The second law or the exergy analysis could be achieved at bulk or at intrinsic (local) level. Relying on the first and second law statement of phenomenological thermodynamics, the bulk level is widely used and, lately, it became a customary part of modern thermodynamic textbooks. The bulk level has many advantages. Among them, the most important are the simplicity, flexibility and the capability to be linked to the mathematical or numerical minimization procedures. The intrinsic approach is trickier since it imposes the use of Navier-Stokes system of equations, which describes, at the continuum level, the velocity and temperature fields. Instead of solving the continuum level extended forms of entropy or exergy equations, these fields are used to directly compute the volumetric rate of entropy generation. By integrating it over the entire flow domain, the overall rate of entropy creation or the overall rate of exergy destruction can be computed. Obviously, this level is more laborious, but it has the great advantage that it reveals the irreversibility by its true mechanism of creation.

Reviewing the state of art of thermodynamic analysis methods, Lior [1] emphasized the necessity of intrinsic approach and established its objectives: (1) identification of the specific phenomena/processes that have large exergy losses or irreversibilities, (2) understanding why these losses occur, (3) evaluation of how they depend on any changes in the process parameters and configuration, and (4) as a consequence of all these, suggestions on how the process could be improved.

In the frame of Lior's statements, the first and second steps were reached. So, for laminar mono-component flows, the volumetric irreversibility is created by viscous and thermal mechanisms [2]-[4]. Although these mechanisms act in turbulent flows too, the turbulence phenomena bring new irreversibility components since the fluctuations generated at the highest turbulence scales are finally dissipated at the smallest ones (Taylor micro-scale) by the fluid diffusivities (kinematic viscosity and thermal diffusivity) [5]. But the third step is still in progress.

Generally, within a complex turbulent flow, some fundamental kind of flows, like boundary layers, mixing jets, wakes and recirculation regions appear together. Each of them has its role in performing the flow task, but it may also have its proper structure of exergy destruction. Therefore, the goal of this paper is to analyze the peculiarities of the exergy destruction structure of some wall bounded and free shear flows, which commonly appear in the complex processes of open thermodynamic systems.

For the sake of clarity, first we will briefly present the bulk and the intrinsic approaches of thermodynamic analysis, and further, establishing the

mathematical model, we shall reveal the numerically simulated structure of the lost exergy.

2. The bulk approach of thermodynamic analysis

Let us consider the thermodynamic system shown in Fig. 1. We suppose that, within the system, no chemical reactions occur. The instantaneous mass, momentum and total energy of the system are M , \vec{J} and E , respectively. The mass, momentum and total energy equations look like:

$$\frac{dM}{d\tau} = \dot{m}_1 - \dot{m}_2 \quad (1)$$

$$\frac{d\vec{J}(\tau)}{d\tau} = (\dot{m}\vec{w} + pA\vec{n})_1 - (\dot{m}\vec{w} + pA\vec{n})_2 + \sum \vec{F}_{ext} \quad (2)$$

$$\frac{dE}{d\tau} = \dot{Q}_{12} - P_{12} + (h_1 + \frac{1}{2}w_1^2 + gy_1)\dot{m}_1 - (h_2 + \frac{1}{2}w_2^2 + gy_2)\dot{m}_2 \quad (3)$$

From the entropy and exergy balance equations we find that:

$$\dot{S}_{gen} = -\frac{dS}{d\tau} - \frac{\dot{Q}_{12}}{T_w} - \dot{m}_1 s_1 + \dot{m}_2 s_2 > 0 \quad (4)$$

$$\dot{I} = \dot{Ex}_Q - \dot{Ex}_P + \dot{Ex}_{h1} - \dot{Ex}_{h2} - \frac{dEx}{d\tau} > 0 \quad (5)$$

where \dot{S}_{gen} represents the rate of entropy generation and \dot{I} is the exergy destruction rate.

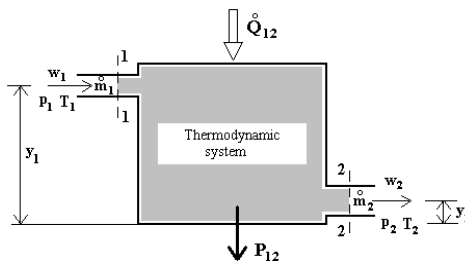


Fig.1 The analysed thermodynamic system

The equations (4)-(5) lay on the bulk thermodynamic methods of analysis, namely second law and exergy analysis, because, based on the equations (1)-(3) they allow computing \dot{S}_{gen} or \dot{I} . Further, by splitting the rate of entropy creation in its viscous and thermal parts (see for example ref. [2]), or the exergy into its kinetic, physical and chemical components [6], one can obtain additional information on the irreversibility exergy destruction mechanisms. The advantage of the bulk methods is undisputed, because, through the number of entropy creation N_s , or the exergy efficiency η_{ex} , they are able to reveal the optimum

operating conditions of thermodynamic processes in the fields of cooling, power generation or refrigeration [7]-[9]. More than that, transforming the lost exergy in its associated cost and adding the costs of purchase, operation, maintenance and depreciation of thermal device, one can perform the thermo-economic analysis [6], [10].

Taking into account that the rate of exergy destruction is linked with the entropy production rate by the well known Gouy-Stodola theorem:

$$\dot{I} = T_0 \dot{S}_{gen} \quad (6)$$

one can observe that in an explicit or implicit manner, all the methods of thermodynamic analysis lie on the rate of entropy generation. But the bulk approach does not allow revealing the true mechanisms of irreversibility creation which drastically decrease the efficiency of all thermodynamic processes.

3. The intrinsic approach of thermodynamic analysis

At the continuum level, the equations (1)-(3) for a turbulent incompressible flow are rewritten as:

$$\frac{\partial \bar{u}_i}{\partial x_i} = 0 \quad (7)$$

$$\frac{\partial(\bar{u}_i)}{\partial \tau} + \frac{\partial}{\partial x_j} \left[\bar{u}_i \bar{u}_j + \frac{\bar{p}}{\rho} \delta_{ij} - \frac{1}{\rho} (\bar{\tau}_{ij} + \bar{\tau}_{ij}^{(t)}) \right] = 0 \quad (8)$$

$$\frac{\partial \bar{T}}{\partial \tau} + \frac{\partial}{\partial x_i} \left[\bar{u}_i \bar{T} + \frac{1}{\rho c_p} (\bar{q}_i + \bar{q}_i^{(t)}) \right] = 0 \quad (9)$$

In the above equations, the following terms appear:

$$\bar{\tau}_{ij} = \mu \left(\frac{\partial \bar{u}_i}{\partial x_j} + \frac{\partial \bar{u}_j}{\partial x_i} \right) ; \quad \bar{q}_{ij} = -\lambda \frac{\partial \bar{T}}{\partial x_i} \quad (10a,b)$$

$$\bar{\tau}_{ij}^{(t)} = -\rho \bar{u}_i \bar{u}'_j ; \quad \bar{q}_i^{(t)} = -\rho c_p \bar{u}'_i \bar{T}' \quad (11a,b)$$

where μ , λ and c_p are the viscosity, thermal conductivity and specific heat at constant pressure, respectively. In the frame of eddy diffusivity models, one can write:

$$\frac{1}{\rho} \bar{\tau}_{ij}^{(t)} = \nu_t \left(\frac{\partial \bar{u}_i}{\partial x_j} + \frac{\partial \bar{u}_j}{\partial x_i} \right) - \frac{2}{3} \delta_{ij} k ; \quad \frac{1}{\rho c_p} \bar{q}_i^{(t)} = -\frac{\lambda_t}{\rho c_p} \frac{\partial \bar{T}}{\partial x_i} = \alpha_t \frac{\partial \bar{T}}{\partial x_i} \quad (12a,b)$$

The turbulent kinematic viscosity, ν_t , and the turbulent thermal diffusivity, α_t , are computed by the aid of turbulent closure models. In this paper we employed the following two models:

1. The ν^2-f model for ν_t [11],[12] combined with the algebraic relation of Rokni și Sunden (RS) for α_t ;

2. The models of Abe-Kondoh and Nagano (AKN) [14], [15] for both v_t and α_t .

All the numerical simulations were performed with the commercial solver FLUENT v6.03. The AKN turbulence model for turbulent momentum is built in the solver. All the others models were implemented by external subroutines. The accuracy of implementations was verified in ref. [16] for v^2 - f and RS models and in ref. [17] for the AKN turbulence model computing the turbulent heat flux.

At the continuum level one can also obtain the balance equations of entropy and exergy (the homologous of eq. (4)-(5)). Theoretically, they describe the irreversibility and the exergy fields. Practically they are useless because, in the frame of eddy viscosity concept, these equations are not closed and consequently they cannot be used for computing the volumetric rate of entropy generation or the volumetric exergy destruction rate. In these conditions, we have to focus on the expression of the volumetric entropy generation rate and on the formulation, at the continuum level, of the Gouy-Stodola theorem.

In the case of turbulent flows the volumetric rate of entropy generation is computed by the following relation [5]:

$$\bar{\sigma} = \bar{\sigma}_{vm} + \bar{\sigma}_{vt} + \bar{\sigma}_{qm} + \bar{\sigma}_{qt} \quad (13)$$

As in the case of laminar flows, the sources of irreversibility are the viscous and thermal phenomena. The corresponding terms are denoted by the subscripts v and q in eq. (13). The structure of irreversibility is more complicated because the two mechanisms of dissipations are happening not only at the large scale of mean flow but also at the smallest scales (Taylor scale) of turbulent fluctuation. These mechanisms of irreversibility creation are denoted by subscripts m and t , respectively.

The relations of mean viscous and mean thermal components of irreversibility are:

$$\bar{\sigma}_{vm} = \frac{\rho}{\bar{T}} (2v \bar{S}_{ij} \bar{S}_{ij}) ; \quad \bar{\sigma}_{qm} = \frac{\lambda}{\bar{T}^2} \frac{\partial \bar{T}}{\partial x_j} \frac{\partial \bar{T}}{\partial x_j} \quad (14,15)$$

The turbulent viscous and turbulent thermal components are expressed by:

$$\bar{\sigma}_{vt} = \frac{\rho}{\bar{T}} (2v \bar{S}'_{ij} \bar{S}'_{ij}) = \frac{\rho \varepsilon}{\bar{T}} ; \quad \bar{\sigma}_{qt} = \frac{k}{\bar{T}^2} \frac{\partial T'}{\partial x_j} \frac{\partial T'}{\partial x_j} = \frac{\rho c_p}{\bar{T}^2} \varepsilon_\theta \quad (16,17)$$

where ε and ε_θ are the dissipation rates of turbulent kinetic energy, $k = \frac{1}{2} \bar{u}'_j \bar{u}'_j$, and half of fluctuating temperature variance, $k_\theta = \frac{1}{2} \bar{T}'^2$, respectively.

In accordance with the Gouy-Stodola theorem, the volumetric rate of each exergy destruction component is computed as:

$$\iota_{(j)} = T_0 \bar{\sigma}_{(j)} \quad (18)$$

where $j=vm, vt, qm$ and qt . By integrating the volumetric rates over the whole flow domain, the overall rate of exergy destruction component is determined:

$$\dot{I}_{(j)} = \iiint_{\Omega} \iota_{(j)} d\Omega = T_0 \iiint_{\Omega} \bar{\sigma}_{(j)} d\Omega = T_0 \dot{S}_{gen}^{(j)} \quad (19)$$

The proportion of each overall component in the whole exergy destruction defines the structure of lost exergy. This structure is quantified by the ratios:

$$\varphi_i = \dot{I}_{(j)}/\dot{I} \quad (20)$$

Knowing their values, one can find the actual ways for improving the exergy efficiency of thermal processes.

The exergy or entropy analyses based on eq. (14)-(20) define the intrinsic methods of thermodynamic analysis. In most cases, the flow solution can not be analytically found, but by applying numerical simulation procedures. This is why, before attaining the intrinsic analysis, one should compare the flow numerical results with available experimental data.

4. The structure of lost exergy in boundary layer

To analyze the structure of exergy losses in boundary layers we have chosen as reference the experimental study of Weighardt and Tillmann [17]. The initial test conditions were: $M_\infty = 0.096$ ($U_\infty = 33.33 \text{ m/s}$) and $K_\infty / m_\infty^2 = 1.4 \times 10^{-5}$. Although the experimental data were obtained for an adiabatic flow, the heat transfer was also considered by imposing as boundary conditions of the numerical simulation the plate wall temperature, $T_w = 350 \text{ K}$, and the inflow air temperature, $T_\infty = 300 \text{ K}$. As the temperature gap $\Delta T = T_w - T_\infty = 50 \text{ K}$ is relatively small, the air viscosity can be considered constant and thus, the energy equation is decoupled from the continuity and momentum equations. Under these considerations, the heat transfer phenomena do not affect the numerical values of the velocity profiles and skin friction coefficient. In order to validate the heat transfer simulation, the Stanton number was computed from the well known Colburn analogy, $St_x = (C_f/2) \cdot Pr^{-2/3}$, where C_f is the experimental skin friction coefficient reported in [17]. For the momentum equations we used the v^2-f turbulence model, while for the energy one we employed the algebraic RS turbulence model. The last one does not allow computing directly ε_θ . To obtain it, we used the following relations:

$$\varepsilon_\theta = \frac{k_\theta}{R_\tau} \frac{\varepsilon_k}{k} \quad (21)$$

where $R_\tau = 0.7$ and k_θ is the solution of the following equation:

$$\frac{\partial}{\partial x_j} \left[\rho \bar{u}_j k_\theta - \rho \left(\alpha + \frac{\alpha_t}{\sigma_\theta} \right) \frac{\partial k_\theta}{\partial x_j} \right] = \rho \left(\alpha_t \frac{\partial \bar{T}}{\partial x_j} \frac{\partial \bar{T}}{\partial x_j} - \frac{k_\theta \varepsilon_k}{k R_\tau} \right) \quad (22)$$

which was implemented in the solver by an external routine.

The numerical results revealed that, at $x=4.987$ m (which is often used as reference for testing the behavior of turbulence models), the differences between the numerical and the experimental values are around 4% for both the skin friction coefficient and the Stanton number. But, while the error of C_{fx} remained in the same range along the plate, the error of Stanton number was growing up towards the plate leading edge, reaching 8.4% at the coordinate $x=0.36$ m. Knowing the difficulties in simulating the turbulent convection heat transfer, one can consider that the results of the numerical simulations are acceptable.

The normal to wall distributions $\iota_{(j)}=\iota_{(j)}(y)$ strongly depend on the x -coordinate. To eliminate this dependence, we expressed the volumetric exergy losses in the term of wall coordinates, resulting:

$$l_{(j)}^+ = \sigma_{(j)} \frac{T_w v}{T_0 u_\tau^2 \tau_w} \quad (23)$$

where τ_w is the wall stress and u_τ represents the friction velocity. The dimensionless distributions $l_{(j)}^+ = l_{(j)}^+(y^+)$ are presented in Fig. 2. Obviously, the ratio between the viscous and thermal components of volumetric exergy dissipations depends on Brinckmann number, which in our case has the value of 0.0164. In this condition, for a comfortable visualization, in Fig. 2 the viscous components were multiplied by a factor of 5.

Figs. 3 shows the structure of overall exergy losses for two lengths of the numerical simulated boundary layer, namely $L=1$ m and $L=6.25$ m.

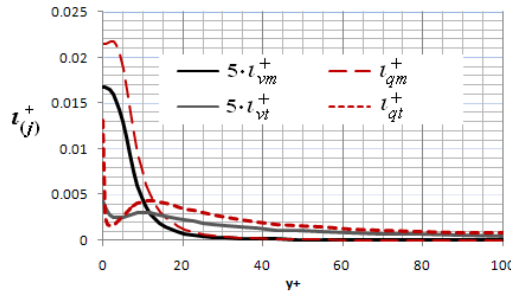


Fig.2. The distribution of volumetric exergy loss on the plate normal direction

As expected, in both cases the percentage of viscous and thermal exergy losses remains constant, namely 11.2% and 88.8% respectively. Their ratio is in accordance to the value of the expression $BrT_w/\Delta T = 0.115$. As one can notice in figure 2, the increase in boundary layer thickness leads to a higher proportion of the turbulent components with respect to the mean ones.

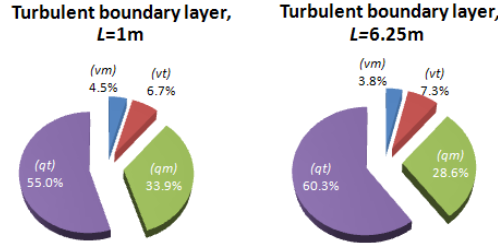


Fig.3 The structure of overall exergy losses in boundary layer.

Thus, the ratio I_{vt}/I_{vm} is 1.49 for 1 m length boundary layer and 1.92 for 6.2 m length, respectively, while the ratio I_{qt}/I_{qm} is 1.62 and 2.1 respectively. Obviously, the increase in boundary layer length (or better said the increase of its thickness) over a certain value involves unjustified exergy losses due to the increase of turbulent dissipations.

5. The structure of exergy losses in turbulent mixing layer

The mixing layers differ from the turbulent wall bounded flow since they are remote from walls and the turbulence is created by the mean velocity difference between the streams. As a result, the exergy losses, especially those concerning the turbulent parts, may have some peculiarities which have to be investigated. We chose for that the plane mixing layer experimentally studied in [18]. The flow geometry is shown in Fig. 4.

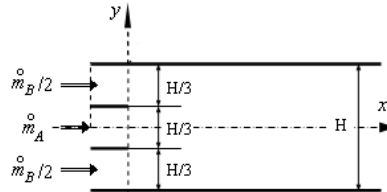


Fig. 4 The flow geometry of mixing layer

The centerline velocity and bulk temperature in the inlet section of central stream are $U_{0A}=108.9$ m/s and $T_{0A}=403.01$ K, respectively. The companion stream enters in the mixing region with a centerline velocity $U_{0B}=73.5$ m/s and a bulk temperature $T_{0B}=314.3$ K. It is well known that the accuracy of the numerical simulation (especially in the case of temperature field) strongly depends on the right selection of the inlet profiles of the flow quantities, such as velocity, turbulent kinetic energy and turbulent dissipation rate. Some of them were not measured near the inflow boundary. So, in order to obtain these profiles as close as possible to the experimental conditions, the computing domain of the two

initial separated streams was extended with 0.5 m in upstream flow direction. The turbulent momentum and turbulent heat were modeled with AKN turbulence models.

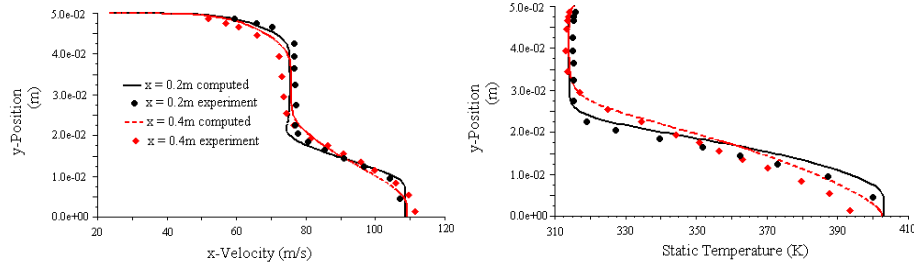


Fig. 5. The computed and measured distributions of velocity and temperature in mixing layer

Figs. 5 present the computed and the measured cross stream profiles of mean velocity and mean temperature at two stream-wise locations, $x=0.2\text{m}$ and $x=0.4\text{m}$. The numerical velocity profiles are in good agreement with the experimental ones. The computed profiles of temperature match the experimental data only in the upper half of the characteristic flow width. Towards the flow centerline, the errors are higher and increase in downstream direction. However, taking into account the difficulties of $k-\epsilon$ turbulence models to predict the spreading rates and the correct levels of turbulent kinetic energy in the jets and mixing layers, we can consider the results of the numerical simulation as acceptable.

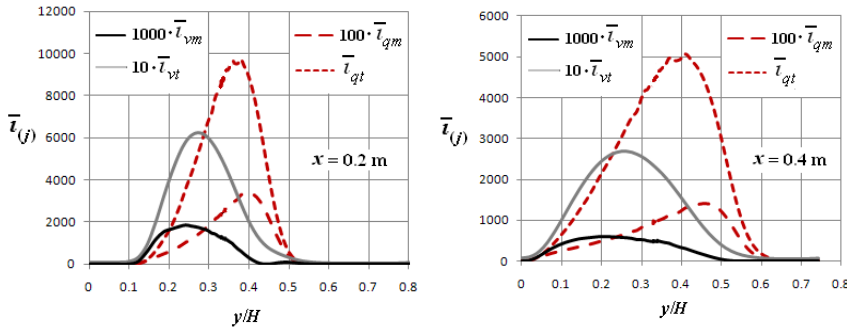


Fig. 6 The distributions of volumetric exergy losses in mixing layer

When trying to find a dimensionless form of $\iota_{(j)}$, the wall coordinates are obviously useless. Thus, we have to choose a characteristic scale of the volumetric exergy losses, which may be expressed as:

$$\iota_{Ch} = \frac{\lambda T_0}{H^2} \left(\frac{2\Delta T}{T_{0A} + T_{0B}} \right)^2 \quad (24)$$

Using it, the dimensionless distributions of volumetric exergy losses are computed with the expression:

$$\bar{\tau}_{(j)} = \tau_{(j)} / \tau_{Ch} \quad (25)$$

and are shown in Fig. 6. As expected, the volumetric exergy losses occur in the mixing region of the two streams. Practically, the boundaries of mixing zone could be identified by the aid of these distributions, which basically have the same shape. The differences among them appear in the location of their peaks and in the peak values. Clearly, the gap between the viscous and thermal components is imposed by the inflow boundary conditions of the two streams, but the difference between the turbulent and the mean components of viscous or thermal mechanisms of exergy dissipation is huge. One can see that the maximum values of the turbulent component are more than one hundred times greater than the maximum values of mean corresponding components.

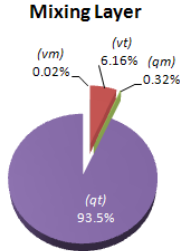


Fig. 7 The structure of overall lost exergy in mixing layer

The computed structure of overall exergy losses shown in Fig. 7 confirms the above statements. The ratios I_{vt}/I_{vm} and I_{qt}/I_{qm} are 308 and 292, respectively. As the mean mechanisms of exergy loss represent only 0.34% from the whole dissipation, they are negligible in this process.

6. The structure of lost exergy in wake

Although the wakes belong to the class of free shear flows too, their dynamics is quite different from the mixing layers [19]. In this case, the mean momentum is mainly transferred only in downstream direction. This behavior affects the length scales of turbulent eddy, which are higher than those of the turbulent eddies generated in the mixing layers. So, it appears interesting to investigate the structure of exergy loss for this kind of flows.

The wake was separated from the computational domain built for the numerical simulation of the flow and convective heat transfer over the cylinder, experimentally investigated by Sholten and Murray [20]. Even if the numerical simulation was performed in steady state conditions, the agreement between the numerical and experimental Nusselt numbers on the cylinder surface at $Re=21580$ was very good. Unfortunately, in the absence of experimental data in the wake,

the accuracy of the numerical simulation was not verified. Taking into account the grid quality, which was twice adapted, the errors of the numerical prediction are mainly due to the turbulence model. Of course, the heat transfer in the wake, which is determined by the temperature differences appearing downstream the cylinder, is poor.

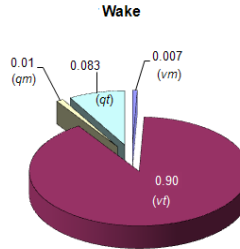


Fig 8. The structure of overall exergy loss in the wake

Fig. 8 presents the structure of the overall exergy loss in this wake. As expected, the turbulent components greatly exceed the mean ones. But the ratios between the turbulent and mean components of the same kind of exergy destruction mechanisms differ by an order of magnitude ($I_{vt}/I_{vm} = 128$ and $I_{qt}/I_{qm} = 8.3$). Comparing to the mean one, the turbulent thermal mechanism is less important than in the previous case. This is happening because of the small temperature gap in the cross-stream wake direction, where the momentum transfer is also negligible.

6. Conclusions

In this paper we have investigated the loss exergy structure of 2D wall bounded and free shear flows. The numerical simulations, performed with the commercial solver FLUENT v. 6.3.12, in which some modern turbulence models for momentum and heat fluxes were implemented, revealed that, in the case of wall bounded shear flows the mean components of irreversibility play an important role in the exergy destruction balance, because they greatly prevail in the viscous sublayer. Their role is diminishing as the length of wall bounded flow is increasing. In the case of free shear flows, like mixing layers and wakes, almost all the exergy dissipations are performed by the specific turbulence irreversibility mechanisms. These results could help in the future for improving the exergy efficiency of thermal processes by operating regimes and geometrical shape modifications.

Acknowledgments

This work is supported by Romanian National Council of University Scientific Research (CNCSIS), Grant 727/2009, named *Intrinsic methods of thermodynamic analysis*.

R E F E R E N C E S

- [1] *N. Lior, W.S. Darkin, H.S. Al-Sharquawi*, The exergy fields in transport processes: Their calculation and use, *Energy*, **31** (2006), 553-578.
- [2] *A. Bejan*, Entropy Generation Minimization, CRC Press, Boca Raton, NY, 1996
- [3] *S. Mahmud, R.A. Fraser*, The second law analysis in fundamental convective heat transfer problems, *International Journal of Thermal Sciences*, **42**(2003), 177-186.
- [4] *R.B. Mansour, N. Galemis, C.T. Nguyen*, Dissipation and Entropy Generation in Fully developed Forced and Mixed Laminar Convection, *International Journal of Thermal Sciences*, **45**(2006), 998-1007.
- [5] *D. Stanciu, M. Marinescu*, Irreversibility Field in Turbulent Heat Convection Problems, *Oil&Gas Science and Technology*, **61**(2006), 191-201.
- [6] *A. Bejan, G. Tsatsaronis, M.J. Moran*, Optimization and thermal design, John Wiley&Sons, 1996.
- [7] *W.A Khan, J.R. Culham, M.M. Yovanovich*, Optimal Design of Tube Bank in Crossflow using Entropy Generation Minimization Method, *J. Thermophysics and Heat Transfer*, **21**(2007) , 372-378.
- [8] *D. Stanciu, Al. Dobrovicescu*, Second Law based Optimisation of Internal Forced Convection through a Duct, *UPB Sci. Bull. Series D, Mechanical Engineering*, **71**, 2, (2009), 79-94.
- [9] *A. Khalil, S.C. Kansik*, Second law based thermodynamic analysis of Brayton/Rankine combined power cycle with reheat, *Applied Energy*, **78** (2004), 179-197
- [10] *Al. Dobrovicescu, D. Stanciu, C. Petre, S. Dorovicescu, G. Târcă-Dragomirescu*, Analysis and optimization of energy systems based on exergoeconomics principles, *Metalurgia International* (in press)
- [11] *F.S. Lien, G. Kalitzin, P.A. Durbin*, RANS modeling for compressible and transitional flows, *Annual Research Brifs, Center for Turbulence Research*, (1998), 267-286
- [12] *A. Sveningsson, L. Davidson*, Assesment of realizability constraint in v^2-f turbulence models, *Int. J. Heat and Fluid Flow*, **25** (2004), 785-794
- [13] *M. Rokni, B. Sundén*, Investigation of a Two-Equation Turbulent Heat Transfer Model Applied to Ducts, *J. Heat Transfer* **125** (2003), 194-200
- [14] *K. Abe, T. Kondoh, Y. Nagano*, A New Turbulence Model for Predicting Fluid Flow anf Heat Transfer in Separating and Reattaching flows-I. Flow Field Calculation, *Int. J. Heat Mass Transfer*, **37** (1994), 1467-1481
- [15] *K. Abe, T. Kondoh, Y. Nagano*, A New Turbulence Model for Predicting Fluid Flow anf Heat Transfer in Separating and Reattaching flows-II. Thermal Field Calculation, *Int. J. Heat Mass Transfer*, **38** (1995), 1467-1481
- [16] *D. Stanciu, Al. Dobrovicescu*, Numerical prediction of heat transfer on transonic turbines blades at off design operating conditions, *UPB Sci. Bull. Series D, Mechanical Engineering*, **71**, 1, (2009), 33-44
- [17] *K. Weighardt, W. Tillmann*, On the turbulent friction layer for rising pressure, *NACA Technical Memorandum 1314*, 1951
- [18] *S. Dimitriu*, Cercetări privind modelarea și simularea numerică a jeturilor de gaze, (Research on modeling and numerical simulation of gas jets), PhD thesis, UPB, 2009 (in Romanian).
- [19] *H. Tennekes, J.L. Lumley*, A first course in turbulence, MIT Press, 1972
- [20] *J.W. Scholten, D.B. Murray*, Unsteady Heat Transfer and Velocity of a Cylinder in Cross Flow –I, Low Freestream Turbulence, *Int. J. Heat and Mass Transfer*, **41** (1998), 1139-1148.